West East High Speed Flow Fields 2002
D. E. Zeitoun, J. Periaux, J. A. Désidéri and M. Marini (Eds.)

PERFORMANCE OF TURBULENCE CLOSURES IN UNSTEADY HIGH SPEED FLOWS

George N. Barakos*
Computational Fluid Dynamics Group
Department of Aerospace Engineering
University of Glasgow
Glasgow G12 8QQ, UK
Email: gbarakos@aero.gla.ac.uk
web page: www.aero.gla.ac.uk/Research/CFD/

Ken J. Badcock
Computational Fluid Dynamics Group
Department of Aerospace Engineering
University of Glasgow
Glasgow G12 8QQ, UK
Email: gnaa36@aero.gla.ac.uk
web page: www.aero.gla.ac.uk/Research/CFD/

Abstract. A review is presented of the current status of turbulence closures employed in unsteady aerodynamic flows. The specific nature of the unsteady flow encountered in the vicinity of lifting surfaces is first considered and the requirements of the turbulence closures are outlined. Several closures are examined and assessed in unsteady flows ranging form dynamic stall cases of oscillating aerofoils to fluttering wings.

Key words: unsteady flow, turbulence modelling, oscillating aerofoils, fluttering wings.

1 INTRODUCTION

In the context of aerodynamics, the numerical simulation of unsteady, turbulent high-speed flows is fuelled by the industrial need to understand flow phenomena associated with the behaviour of aircraft during manoeuvres, as well as flows around helicopter rotors and turbomachinery blades. The flow phenomena appearing in these applications are non-linear due to the presence of separation, unsteadiness, shock/boundary-layer, viscous/inviscid, vortex/body and vortex/vortex interactions, transition to turbulence and flow re-laminarisation. Better understanding of the flow physics associated with all these phenomena creates opportunities for flow control and, subsequently, enhancement of the performance of airplanes and helicopters.

The cost of performing wind tunnel or flight experiments in unsteady flows is very high. Moreover, the information obtained through experiments is usually limited - due to the instrumentation constraints - to pressure distributions or aerodynamic coefficients and to just integral loads for high Mach number 3-dimensional cases. Numerical simulation of unsteady flows is a promising alternative, but it is not free of shortcomings and difficulties; these are primarily related to numerical and turbulence modelling limitations. This work mainly focuses on the problems associated with

turbulence modelling though it also highlights the need of accurate and efficient CFD algorithms, as well as, the need of high quality experimental data for unsteady flow cases.

In view of the above, the objectives of this study are: (i) To provide a pool of validation results for existing turbulence models in unsteady flow conditions. (ii) To identify the weaknesses of the models in terms of accuracy of results, robustness and CPU-time. (iii) To identify promising turbulence modelling approaches for predicting unsteady flows to engineering accuracy.

2 NUMERICAL METHOD

A control volume, time-marching scheme is employed in this work for the solution of the governing equations. The scheme is based on an implicit HLLC solver and a strongly coupled discretisation of the Navier-Stokes and turbulence transport equations. Such a scheme was found to result in better efficiencies than segregated and loosely-coupled time-marching solvers. Source terms appearing in the transport equations of turbulence models are linearised and treated implicitly to improve the stability of the scheme and allow CFL numbers of about 50 to be used. The solver incorporates a variety of turbulence closures ranging from simple algebraic models to anisotropic closures[1] and Detached Eddy Simulation.[2]

3 TURBULENCE MODELLING

For slow varying flow, or flows with a steady mean field, the Reynolds-Averaged Navier-Stokes (RANS) approach is adopted. This approach decomposes the instantaneous turbulent flow field according to:

$$\mathbf{u}(\mathbf{x},t) =< \mathbf{u}(\mathbf{x},t) > +\mathbf{u}'(\mathbf{x},t) \tag{1}$$

where the fluctuating part (indicated by a prime) is modelled using one, two, or even three-equation Eddy-Viscosity Models (EVMs). The above approach is not the preferred one for flows with a rapidly varying mean component or for flows with large organised unsteady structures. Since, numerical modelling of unsteady flows is the primary concern of this work, a different approach should be taken. A common way of extending RANS to unsteady flows is based on the following decomposition:

$$\mathbf{u}(\mathbf{x},t) = \overline{\mathbf{u}}(\mathbf{x}) + < \mathbf{u}(\mathbf{x},t) >_c +\mathbf{u}'(\mathbf{x},t) \tag{2}$$

where the first term represents the mean value of the flow, the second the resolved part of the unsteady flow component and the third term the turbulent fluctuation. In slightly different terms, one may see the second term as the contribution of the coherent flow modes to the dynamics of the flow field and the third term as the random part of the turbulent field. Many different names have been used for this approach with the most common been: Unsteady Reynolds-Averaged Numerical Simulation (URANS) and Very Large Eddy Simulation (VLES). Again, the fluctuation part of the flow field is modelled using various eddy-viscosity models. Clearly, the Large Eddy Simulation approach (LES) is better suited for these flows, however, the penalty one has to pay in terms of CPU time is significant and the application of LES is still restricted to relatively low Reynolds number flow cases.

In this work several eddy-viscosity models have been employed. For the purpose of this paper we classify them as linear and non-linear ones according to the relationship

used to derive the components of the Reynolds stress tensor from the mean strain and vorticity of the flow.
In the case of linear eddy-viscosity models (LEVM) the stress tensor τ_{ij} is modeled using the approximation $\tau_{ij} = \tau_{ij}^l + \tau_{ij}^R$ where τ_{ij}^l is the Newtonian stress tensor,

$$\tau_{ij}^R = \mu_T \left(\frac{\partial u_i}{\partial x_j} + \frac{\partial u_j}{\partial x_i} \right) - \frac{2}{3}\mu_T \frac{\partial u_k}{\partial x_k}\delta_{ij} - \frac{2}{3}\rho k \delta_{ij}$$

is the Boussiesq approximation to the Reynolds stress tensor and μ_T is the eddy-viscosity.
Non-linear eddy-viscosity models (NLEVM) use an expansion of the Reynolds stress components in terms of the mean strain and rotation tensors:

$$S_{ij} = \left(U_{i,j} + U_{j,i}\right)/2, \quad \Omega_{ij} = \left(U_{i,j} - U_{j,i}\right)/2 \tag{3}$$

For the $k-\epsilon$ non-linear EVM by Craft *et al.*,[1] the following cubic expansion of the anisotropy of the Reynolds stress tensor ($a_{ij} \equiv \frac{\overline{u_i u_j}}{k} - \frac{2}{3}\delta_{ij}$) has been suggested:

$$\begin{aligned} a_{ij} = &-\frac{\mu_T}{\rho k} S_{ij} + c_1 \frac{\mu_T}{\rho\tilde{\epsilon}} \left(S_{ik}S_{kj} - \frac{1}{3} S_{kl}S_{kl}\delta_{ij} \right) + c_2 \frac{\mu_T}{\rho\tilde{\epsilon}} \left(\Omega_{ik}S_{kj} + \Omega_{jk}S_{ki} \right) \\ &+ c_3 \frac{\mu_T}{\rho\tilde{\epsilon}} \left(\Omega_{ik}\Omega_{jk} - \frac{1}{3}\Omega_{lk}\Omega_{lk}\delta_{ij} \right) + c_4 \frac{\mu_T k}{\rho\tilde{\epsilon}^2} \left(S_{ki}\Omega_{lj} + S_{kj}\Omega_{li} \right) S_{kl} \\ &+ c_5 \frac{\mu_T k}{\rho\tilde{\epsilon}^2} \left(\Omega_{il}\Omega_{lm}S_{mj} + S_{il}\Omega_{lm}\Omega_{mj} - \frac{2}{3} S_{lm}\Omega_{mn}\Omega_{nl}\delta_{ij} \right) \\ &+ c_6 \frac{\mu_T k}{\rho\tilde{\epsilon}^2} S_{ij}S_{kl}S_{kl} + c_7 \frac{\mu_T k}{\rho\tilde{\epsilon}^2} S_{ij}\Omega_{kl}\Omega_{kl} \end{aligned} \tag{4}$$

This cubic expansion is utilized here to calculate the components of the Reynolds-stress tensor $-\overline{\rho}\ \overline{u_i u_j}$, while the coefficients c_i take the values: $c_1 = -0.1$, $c_2 = 0.1$, $c_3 = 0.26$, $c_4 = -10c_\mu$, $c_5 = 0$, $c_6 = -5c_\mu^2$, $c_7 = -c_6$. The eddy viscosity is calculated by: $\mu_T = c_\mu \rho f_\mu \frac{k^2}{\tilde{\epsilon}}$, where

$$c_\mu = \frac{0.3\left[1 - exp\left\{-0.36exp\left(0.75\eta\right)\right\}\right]}{1 + 0.35\eta^{1.5}}, \quad f_\mu = 1 - exp\left\{ -\left(\frac{\tilde{R}_t}{90}\right)^{1/2} - \left(\frac{\tilde{R}_t}{400}\right)^2 \right\} \tag{5}$$

$$\eta = max\left(\tilde{S}, \tilde{\Omega}\right), \quad \tilde{S} \equiv \frac{k}{\tilde{\epsilon}}\sqrt{S_{ij}S_{ij}/2}, \quad \tilde{\Omega} \equiv \frac{k}{\tilde{\epsilon}}\sqrt{\Omega_{ij}\Omega_{ij}/2}. \tag{6}$$

Functional forms of c_μ (like the one presented above) were found to be beneficial in flows far from equilibrium and similar conclusions have also been reported, for a variety of steady compressible flows.[3] More details about the closure coefficients of this non-linear model as well as the employed near-wall formulation can be found in the work by Craft *et al.*[1] A $k-\omega$ version of the same non-linear eddy-viscosity model is also available.[4]

According to Fan *et al.*,[5] for turbulent flows far from equilibrium, like the unsteady flows investigated in the present paper, it is suggested to avoid the use of the y^+ parameter ($y^+ = \frac{y\rho u_\tau}{\mu}$, where y is the distance from the solid boundary and u_τ is the friction velocity) in the near-wall formulation of the turbulence models.

Instead, the turbulent Reynolds number or, alternatively, the near-wall Reynolds number should be used. In view of the above, the following LEVMs have been employed in this study: i) the one-equation turbulence model of Spalart and Allmaras (SA),[6] ii) the linear low-Re $k-\epsilon$ EVMs of Launder and Sharma (LS)[7] and Fan, Lakshminarayana & Barnett (FLB).[5] The NLEVM by Craft *et al.*[1] was also employed. This is a low-Re, cubic non-linear eddy viscosity model and was mainly applied to steady incompressible flows.[1] Additional results for steady shock/boundary-layer interaction cases have been discussed in.[8] Although in this study we do not aim to carry out a detailed investigation of second-moment closures, some comparisons between the Launder-Shima[9] Reynolds-stress transport model (RSTM) and the EVM models, were also attempted.

4 RESULTS AND DISCUSSION

4.1 Steady State Flow Cases

There have been several validation exercises aiming to assess the performance of turbulence closures in steady high-speed flows. These efforts include CEC projects, like EUROVAL,[10] ETMA[11] and ECARP, as well as individual efforts like the ones undertaken by Bardina *et al.*,[12] among others. An overall conclusion is that for steady-state cases, advanced turbulence closures were able to provide adequate predictions. Results obtained for several flow cases demonstrate that, in complex strain associated with curvature, swirl, separation and rapid change of flow direction, the anisotropic closures often return superior performance to that of isotropic eddy-viscosity models. Figure 1 presents indicative results for the flow over a compression ramp at 24° angle ($Re = 6.3 \times 10^7$, $M = 2.79$).[13] Better agreement between experiment and simulation is obtained by using a non-linear eddy-viscosity model.[1] In particular, the sharp rise of the pressure is predicted very close to the experimental data and the pressure plateau corresponding to the separation near the corner of the ramp is of about the same length as the experimental one. The same good agreement has been reported[8] for several other cases including the well-known shock/boundary-layer interaction case by Delery.[14]

4.2 Unsteady Flow Cases

This success still holds for certain unsteady cases with moderate separation and slow varying mean-flow values. Figure 2(a) presents the hysteresis of the aerodynamic loads for a harmonically oscillating aerofoil case. This case known as the AGARD CT-1 test,[15] is well predicted even with simple 1-eq closures. The case concerns the unsteady, transonic flow around a NACA-0012 aerofoil with Mach and Reynolds numbers of 0.6 and 4.8×10^6, respectively. The mean incidence angle is 2.8° and the amplitude of oscillation is 2.4°. The aerofoil performs pitching motion with respect to the quarter-chord axis ($x/c = 0.25$) at a reduced frequency of 0.16. The results for the lift loop are shown in Fig. 2(a) for the linear EVM model of Fan *et al.*[5] (FLB), the NLEVM of Craft *et al.*[1] and the RSTM of Launder & Shima.[9] However, the flow unsteadiness is mainly dictated by the small amplitude oscillations of the body and the response of the boundary layer. During the oscillation cycle the flow remains attached.

Figure 3 presents the position of the shock wave during the shock-induced oscillation of the 18% circular-arc aerofoil. The experiments for this case were performed by McDevitt and Levy[16] and represent a textbook example of transonic buffet. Fig-

ure 4 shows the instantaneous Mach number contours. The motion of the shock over about 50% of the chord is well predicted. The same is true for the extent of the separated flow region near the trailing edge of the profile. In this case, the unsteadiness of the large flow structures appears to play a secondary role in the development of the turbulent flow field. In addition, the extent of the separated flow regions is moderate and their motion has a time scale much larger than turbulent fluctuations. For the above two reasons, URANS remains a valid alternative for engineering calculation under the particular flow conditions.

The performance of the models tends to deteriorate for cases with extended separated flow regions. Figure 2(b) presents the loop of the lift coefficient for an oscillating NACA-0012 aerofoil at deep-stall conditions. In contrast to the results for the CT1 case (Figure 2(a)), the NLEVM (labelled NL in the plot) now provides significantly better results than the linear model. The numerical results are compared with experimental data of McAlister *et al.*[17] The free stream Reynolds and Mach numbers are 10^6 and 0.2, respectively. The oscillation amplitude is 10° around a mean incidence angle of 15°, and the reduced frequency of the oscillation is $k_f = 0.25$. The failure of the linear model is due to the fact that it leads to an excessive production of turbulence that inhibits flow separation, thus resulting in poor predictions of the lift and moment loops. In this case, a better prediction has been obtained using the non-linear eddy-viscosity model. In summary the predictions of the non-linear model (NL) appear to be in a better agreement with the experiments though there is still room for improvements. The rich flow field of this particular case is shown in Figure 5 where the dynamic stall vortex is well predicted. The evolution of this field is in agreement with the available experimental data[8] though the predicted aerodynamic loads show some discrepancy with the experiments for the highly unsteady phase of the flow re-arrangement as the aerofoil moves from the max incidence to angles bellow the static stall angle.

Although the flow around oscillating aerofoils is of particular importance in the design and analysis of helicopter rotor blades[15,17] it still remains a simple case, compared to flows of engineering importance in aerospace design. A more complex case is shown in Figure 6, where results are presented for the flutter boundary of the AGARD 445.6 wing case[18] obtained with a variety of turbulence models in the context of the URANS method. Numerically, this case is relatively easy to compute. The shock formed on the thin wing at transonic conditions is weak and the boundary layers are attached. The experiments and calculations all deal with small wing deflections at low incidence. Therefore the treatment of turbulence would not be expected to have a large influence on the aerodynamics. This is confirmed by the good agreement of the current turbulent results with previously published Euler results. Given the failure of a variety of modelling and numerical approaches to capture the experimental stability boundaries around sonic conditions there must be a question about the experimental data. It is, however, difficult to establish the reason behind the obtained discrepancies in the region of the transonic dip 6(c). Unsteady pressure measurements on the wing as well as field measurements at the vicinity of the lifting surfaces are necessary for validation purposes. At present, there are a few experimental investigations suitable for CFD and turbulence modelling validation in complex unsteady 2D flows while 3D cases are very scarce.

5 CONCLUSIONS

Having performed computations for several unsteady flow cases with a variety of closures, a summary of conclusions is now attempted.

During this study (as well as in previous ones[5]) it become evident, that since an instantaneous log-law does not in general exist, formulations based on the wall-functions and the equilibrium assumption are not appropriate for unsteady flow computations. In addition, as the frequency of the unsteadiness increases the turbulence becomes more directly affected by the fluctuating mean flow and non-equilibrium effects become important; this part of the turbulent flow physics is not well represented in most of the available closures. Separation often accompanies the unsteady flow and consequently good prediction of the separated flow region is essential for realistic unsteady flow computations. Regarding the assessed turbulence closures, it was found that for many cases the obtained results were in qualitative agreement with the experiments but quantitative comparisons indicated that there is significant room for improvement. Finally, problems arise from the lack of adequate experimental data for comparison, especially for unsteady flow cases. This is mainly due to the difficulties in performing flow field visualisation and measurements under unsteady flow conditions. There is, however, a need for high quality experiments at realistic Reynolds and Mach numbers in order to assess and possibly "tune" the available turbulence models.

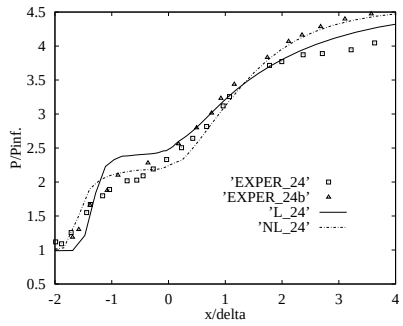

Figure 1: Surface pressure distribution predicted using linear (L) and non-linear (NL) EVMs for the compressible ramp case.[13]

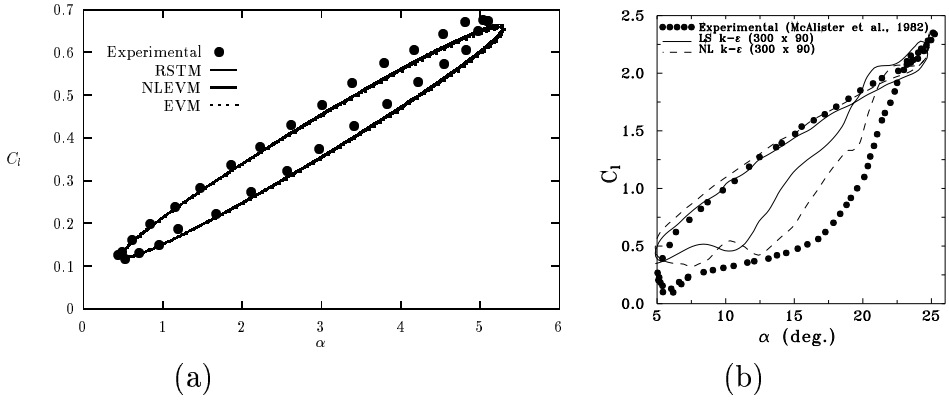

Figure 2: (a) Hysteresis of the aerodynamic loads for the oscillating NACA-0012 aerofoil, AGARD CT1 case.[15] $M = 0.6$, $Re_c = 4.8 \times 10^6$, $k_f = 0.16$, $\alpha_0 = 2.8°$, $\alpha_1 = 2.4°$, $(x/c)_{rot} = 0.25$, $(x/c)_{trip} = 0.1$. (b) Unsteady aerodynamic loads during deep-stall oscillation of a NACA-0012 aerofoil.[17] $M = 0.2$, $Re_c = 10^6$, $k_f = 0.2$, $\alpha_0 = 15°$, $\alpha_1 = 10°$, $(x/c)_{rot} = 0.25$, $(x/c)_{trip} = 0.1$.

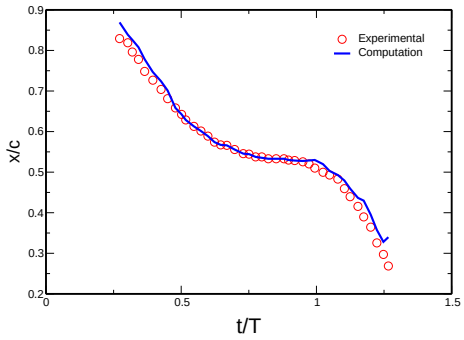

Figure 3: Shock position on the surface of the 18% circular arc aerofoil and comparison with the experiments of McDevitt and Levy.[16]

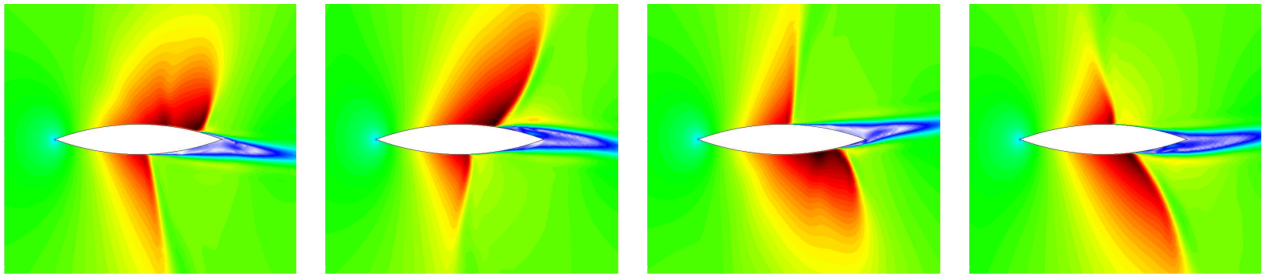

Figure 4: Mach number field around the 18% circular arc aerofoil during the SIO. The flow case corresponds to the experiments by McDevitt and Levy.[16]

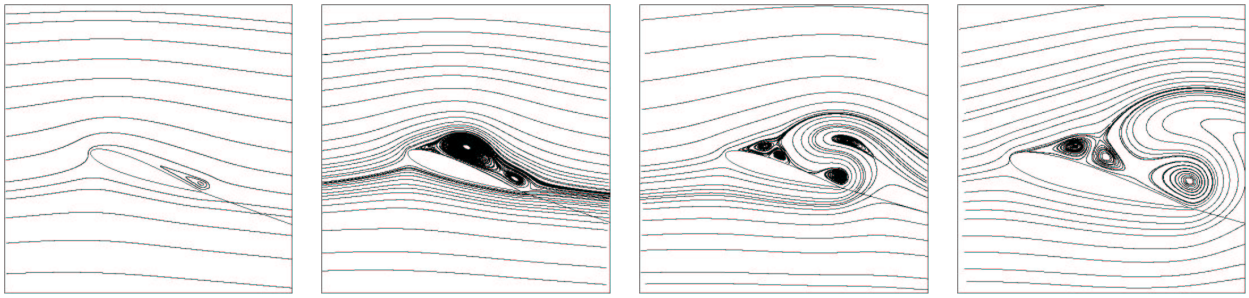

Figure 5: Unsteady flow field during deep-stall oscillation of a NACA-0012 aerofoil.[17] $M = 0.2$, $Re_c = 10^6$, $k_f = 0.2$, $\alpha_0 = 15°$, $\alpha_1 = 10°$, $(x/c)_{rot} = 0.25$, $(x/c)_{trip} = 0.1$.

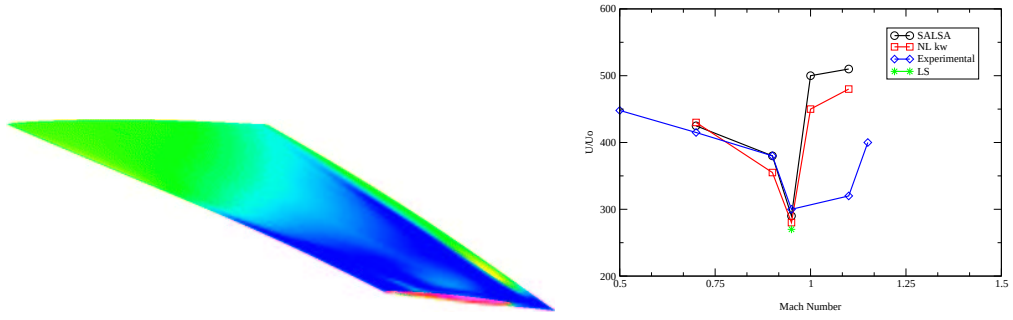

(a) (b)

Figure 6: (a) fluttering AGARD 445.6 wing,[18] (b) flutter boundary predicted using various turbulence closures.

REFERENCES

[1] T.J. Craft, B.E. Launder & K. Suga, "Development and Application of a Cubic Eddy-Viscosity Model of Turbulence", *Int. J. Heat Fluid Flow*, **17**, 108-115 (1996).

[2] Nikitin et al., "An Approach to Wall Modelling in Large-Eddy Simulations", *Physics of Fluids*, **12**, 1629-1631 (2000).

[3] M.A. Cotton & J. Ismael, "Some Results for Homogeneous Shear Flows Computed Using a Strain Parameter Model of Turbulence", *Tenth Symposium on Turbulent Shear Flows, TSF-10*, Pennsylvania State University, 26-7–26-12 (1995).

[4] D. Sofialidis & P. Prinos, "Development of a Non-Linear Strain-Sensitive $k-\omega$ Turbulence Model", *Eleventh Symposium on Turbulent Shear Flows, TSF-11*, Grenoble France, 2-89–2-94 (1997).

[5] S. Fan, B. Lakshminarayana, & M. Barnett, "Low-Reynolds-Number $k-\epsilon$ Model for Unsteady Turbulent Boundary-Layer Flows", *AIAA J.*, **31**, 1777-1784 (1993).

[6] P.R. Spalart & S. R. Allmaras, "A One-Equation Turbulence Model for Aerodynamic Flows", *AIAA Paper 92-0439* (1992).

[7] B.E. Launder & B.I. Sharma, "Application of the Energy-Dissipation Model of Turbulence to the Calculation of Flow Near a Spinning Disk", *Letters in Heat and Mass Transfer*, **1**, 131-138 (1974).

[8] G. Barakos & D. Drikakis, "Investigation of Non-Linear Eddy-Viscosity Turbulence Models in Shock-Boundary Layer Interaction", *AIAA J.*, **38**, 461-469 (2000).

[9] B.E. Launder & N. Shima, "Second-Moment Closure for the Near-Wall Sublayer: Development and Application", *AIAA J.*, **27**, 1319-1325 (1989).

[10] W. Haase, F. Brandsma, E. Elsholz, M.A. Leschziner, & D. Schwamborn, *Results of the EC/BRITE-EURAM Project EUROVAL, 1990-1992*, Notes on Numerical Fluid Mechanics, Vol. 42, Vieweg (1993).

[11] A. Dervieux, F. Braza, and J-P. Dussauge, *Computation and Comparison of Efficient Turbulence Models for Aeronautics - European Research Project ETMA*, Notes on Numerical Fluid Mechanics, Vol. 65, Vieweg (1998).

[12] J.E. Bardina, P.G. Huang & T.J. Coakley, "Turbulence Modeling Validation, Testing, and Development", *NASA TM-110446* (1997).

[13] A.J. Smits & K.-C. Muck, "Experimental Study of Three Shock Wave/Turbulent Boundary Layer Interactions", *J. Fluid Mech.*, **182**, 291-314 (1987).

[14] J. Delery, "Investigation of Strong Turbulent Boundary-Layer Interaction in 2D Flows with Emphasis on Turbulence Phenomena", *AIAA 81-1245* (1981).

[15] *Compendium of unsteady aerodynamic measurements*, AGARD Advisory Report No. 702, AGARD (1983).

[16] J.B. McDevitt, L.L. Levy Jr., & G.S. Deiwert, "Transonic Flow about a Thick Circular-Arc Airfoil", *AIAA J.* **14**, 606-613 (1976).

[17] K.W. McAlister, S.L. Pucci, W.J. McCroskey & L.W. Carr, "An experimental study of dynamic stall on advanced airfoil sections. Volume 2: pressure and force data", *NASA Technical Memorandum 84245* (1982).

[18] E.C. Yates, "AGARD Standard Aeroelastic Configurations for Dynamic Response I: Wing 445.6", *AGARD Advisory Report No. 765*, AGARD (1988).